IIW Doc. V- 1523 -12
Tatsuya YOSHIMOTO[1], Hideki HORIKAWA[1], Takumi SUGIOKA[1], Yoji WADA[1], Tomiko YAMAGUCH[2] and Kazumasa NISHIO[2]

METHOD TO CALCULATE ULTRASONIC WAVE VELOCITY BY USING CHEMICAL COMPOSITION OF AUSTENITIC STAINLESS STEELS
METODE IZRAČUNAVANJA BRZINE ULTRAZVUČNIH TALASA KORIŠĆENJEM HEMIJSKOG SASTAVA AUSTENITNOG NERĐAJUĆEG ČELIKA

NASTAVAK IZ PREDHODNOG BROJA
2.deo

3.6.2 Partial differential equation

Equations (1) and (2) were partially differentiated with respect to each parameter *E*, *v*, and *ρ* to simulate a deviation in ultrasonic wave velocity coused by a deviation in each parameter.

Partial differentiation of Eq. (1) with regard to *E* gives Eq. (9).

$$\frac{\partial C_L}{\partial E}=\frac{1}{2}\left(\frac{(1-\nu)}{\rho(1+\nu)(1-2\nu)}\right)^{1/2}\frac{1}{E^{1/2}} \qquad (9)$$

Partial differentiation of Eq. (1) with regard to *v*givesEq. (10).

$$\frac{\partial C_L}{\partial \nu}=\left(\frac{E}{\rho}\right)^{1/2}\left(\frac{\nu(2-\nu)}{(1-\nu)(1+\nu)^3(1-2\nu)^3}\right)^{1/2} \qquad (10)$$

Partial differentiation of Eq. (1) with regard to *ρ* gives Eq. (11).

$$\frac{\partial C_L}{\partial \rho}=-\frac{1}{2}\left(\frac{E(1-\nu)}{(1+\nu)(1-2\nu)}\right)^{1/2}\rho^{-3/2} \qquad (11)$$

Partial differentiation of Eq. (2) with regard to *E* gives Eq. (12).

$$\frac{\partial C_S}{\partial E}=\frac{\sqrt{2}}{4}\left(\frac{1}{\rho(1+\nu)}\right)^{1/2}E^{(-1/2)} \qquad (12)$$

Partial differentiation of Eq. (2) with regard to *v*gives Eq. (13).

$$\frac{\partial C_S}{\partial \nu}=-\frac{\sqrt{2}}{4}\left(\frac{E}{\rho}\right)^{1/2}(1+\nu)^{(-3/2)} \qquad (13)$$

Partial differentiation of Eq. (2) with regard to density *ρ* gives Eq. (14).

$$\frac{\partial C_S}{\partial \rho}=-\frac{\sqrt{2}}{4}\left(\frac{E}{(1+\nu)}\right)^{1/2}\rho^{(-3/2)} \qquad (14)$$

Moreover, Eq. (6) was partially differentiated with respect to *d* to simulate a deviation in *ρ* coused by a deviation in *d* and Eq. (15) can be given.

$$\frac{\partial \rho}{\partial d}=-\frac{12}{Nd^4}\left(\sum_{i=1}^{n}M_i a_i+\frac{A}{1-A}Mc\right) \qquad (15)$$

CONTINUED FROM PREVIOUS ISSUE
Part 2

3.6.2 Delimične diferencijalne jednačine

Jednačine (1) i (2) su delimično diferencirane u odnosu na svaki parametar *E,v*, i *ρ* da simulira odstupanje u brzine ultrazvučnog talasa usled odstupanja svakog parametra.

Delimična diferencijacija jednačine (1) u odnosu na *E* daje jednačinu (9).

$$\frac{\partial C_L}{\partial E}=\frac{1}{2}\left(\frac{(1-\nu)}{\rho(1+\nu)(1-2\nu)}\right)^{1/2}\frac{1}{E^{1/2}} \qquad (9)$$

Delimična diferencijacija jednačine (1) u odnosu na *v* daje jednačinu (10).

$$\frac{\partial C_L}{\partial \nu}=\left(\frac{E}{\rho}\right)^{1/2}\left(\frac{\nu(2-\nu)}{(1-\nu)(1+\nu)^3(1-2\nu)^3}\right)^{1/2} \qquad (10)$$

Delimična diferencijacija jednačine (1) u odnosu na *ρ* daje jednačinu (11).

$$\frac{\partial C_L}{\partial \rho}=-\frac{1}{2}\left(\frac{E(1-\nu)}{(1+\nu)(1-2\nu)}\right)^{1/2}\rho^{-3/2} \qquad (11)$$

Delimična diferencijacija jednačine (2) u odnosu na *E* daje jednačinu (12).

$$\frac{\partial C_S}{\partial E}=\frac{\sqrt{2}}{4}\left(\frac{1}{\rho(1+\nu)}\right)^{1/2}E^{(-1/2)} \qquad (12)$$

Delimična diferencijacija jednačine (2) u odnosu na *v* daje jednačinu (13).

$$\frac{\partial C_S}{\partial \nu}=-\frac{\sqrt{2}}{4}\left(\frac{E}{\rho}\right)^{1/2}(1+\nu)^{(-3/2)} \qquad (13)$$

Delimična diferencijacija jednačine (2) u odnosu na *ρ* daje jednačinu (14).

$$\frac{\partial C_S}{\partial \rho}=-\frac{\sqrt{2}}{4}\left(\frac{E}{(1+\nu)}\right)^{1/2}\rho^{(-3/2)} \qquad (14)$$

Šta više, jednačina (6) je delimično difrencirana u odnosu na *d* da bi simulirali odstupanje *ρ* uzrokovano odstupanjem *d* i može se dati jednačina (15)

$$\frac{\partial \rho}{\partial d}=-\frac{12}{Nd^4}\left(\sum_{i=1}^{n}M_i a_i+\frac{A}{1-A}Mc\right) \qquad (15)$$

4. Results and Discussions

4.1 Acoustic Anisotropy Concerning Transverse Wave Velocity Ratio

Table 5 shows the measured values of transverse wave velocity ratio. Since transverse wave velocity ratio of T.P.No.1-1 ～ 1-6 is very small, it is evident that acoustic anisotropy for these materials is not observed.

4. Rezultati i diskusija

4.1 Akustična anizotropija u odnosu na odnos brzina transverzalnog talasa

Tabela 5 prikazuje izmerene vrednosti odnos brzine transverzalnog talasa. S obzirom da je odnos brzine transverzalnog talasa za T.P.No.1-1 ~ 1-6 vrlo mali, evidentno je da nije utvrđena akustična anizotropija za ove materijale.

	Dimension	Ref. No.	C	Si	Mn	P	S	Ni	Cr	Mo	Fe
Young's Modulus	GPa	7			198.0			205.0	253.0	327.0	190.0
		11	4.8	113.1	158.6			206.1	248.2	324.1	196.5
		Ave.	4.8	113.1	178.3			205.55	250.6	325.55	193.25
Poisson's Ratio	None	12		0.44	0.24			0.31	0.30	0.30	0.29
		13						0.31	0.21	0.29	0.29
		Ave.		0.44	0.24			0.31	0.255	0.295	0.29
Atomic Weight	None	7	12.01	28.09	54.94	30.97	32.07	58.69	52.00	95.94	55.85
		10	12.01	28.09	54.94	30.97	32.07	58.69	52.00	95.94	55.85
		Ave.	12.01	28.09	54.94	30.97	32.07	58.69	52.00	95.94	55.85

Table 4 *Reference data of Young's modulus, Poisson's ratio and atomic weight of elementary substance*
Tabela 4 *Referentni podaci o Jungovom modulu, Poasonovog odnosa i atomske mase elementarnih supstanci*

T.P. No.	AISI No.	Transverse Wave Volocity Ratio
1-1	304	1.003
1-2	304	1.002
1-3	304	1.000
1-4	304L	1.002
1-5	310S	1.004
1-6	316	1.004

Table 5 *Measured values of transverse wave velocity ratio*
Tabela 5. *Izmerene vrednosti koeficijenta brzine transverzalnog talasa*
transverse wave velocity ratio- odnos brzine transverzalnog talasa

4.2 Measured Values of Density, Young's modulus and Poisson's ratio

Table 6 shows the measured values of ρ, E and v of T.P. No.1-1 ～ 1-6. It was observed that ρ of AISI type 304 stainless steel (T.P.No.1-1 ～ 1-3) and AISI type 304L stainless steel (T.P.No.1-4) slightly decreased with the increase in carbon content, although the concentration of Ni and Cr were almost the same. Error between E measured by ultrasonic testing and one by strain gauge method, was in a range of approximately -2 ～ 3 % as shown in Table 4. Error between v measured by ultrasonic testing and one by strain gauge method was in a range of approximately -5 ～ 5 %. E and v measured by ultrasonic testing were compared with the calculated ones.

4.3 Comparison between Calculated Values and Experimental Ones

4.3.1 Lattice parameter

Fig. 2 shows the relation between experimental values and ones calculated by Eq. (5). In this figure, the calculated values were within an allowable margin of error, (we assumed that a few percent of error could be allowed, based on our experience), when compared with experimental values

4.2 Izmerene vrednosti gustine, Jungovog modula i Poasonovog odnosa

Tabela 6 prikazuje izmerene vrednosti ρ, E i v za T.P. No.1-1 ~ 1-6.

Uočeno je daseρ, kod AISI 304 tipa nerđajućeg čelika (TPNo.1-1 ~ 1-3) i tip 304L nerđajućeg čelika (TPNo.1-4) neznatno smanjio s povećanjem sadržaja ugljenika, iako su koncentracija Ni i Cr bili gotovo isti. Greška između izmerenog E ultrazvučnim ispitivanjem i metodom merača naprezanja, bila je u rasponu od oko -2 ~ 3% kao što je prikazano u tabeli 4. Greška između izmerenih v ultrazvučnim ispitivanjem i metodom merača naprezanja je u rasponu od oko -5 ~ 5%.

E *i* v izmerene ultrazvučnim ispitivanjem su upoređene u odnosu na izračunate vrednosti.

4.3 Poređenje izračunatih i eksperimentalnih vrednosti

4.3.1 Parametar rešetke

Sl. 2 prikazuje odnos između eksperimentalnih vrednosti i izračunatih prema jedn. (5). Na ovoj slici, izračunate vrednosti su bile unutar dozvoljenih margina greške, (pretpostavili smo da nekoliko procenata greška može biti dozvoljeno, na osnovu našeg iskustva), u odnosu na eksperimentalne vrednosti.

4.3.2 Density

Fig. 3 shows the relation between experimental values and the calculated ones of ρ. In this figure, the calculated values were smaller than experimental ones and a margin of error was less than 2.2%. Then we can say that an error coused by the calculation of lattice parameter was within an allowable margin.

4.3.2. Gustina

Sl. 3 prikazuje odnos između eksperimentalnih vrednosti i izračunatih za ρ. Na ovoj slici, izračunate vrednosti su bile manje od eksperimentalnih i margina greške bila je manja od 2,2%. Onda možemo reći da je greška uzrokovana izračunavanjem parametra rešetke unutar dozvoljenih margina.

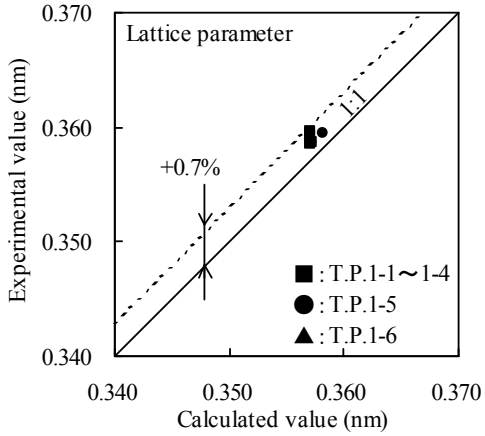

Fig. 2 *Relation between experimental values and calculated ones of lattice parameter*
Sl. 2: *Odnos između eksperimentalnih i izračunatih vrednosti parametra rešetke*

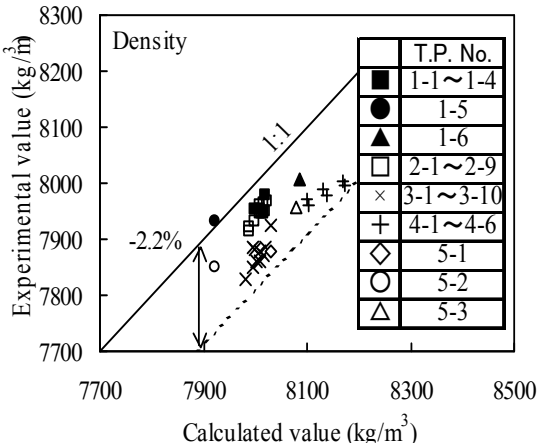

Fig. 3 *Relation between experimental values and calculated ones of density*
Sl. 3: *Odnos između eksperimentalnih i izračunatih vrednosti gustine*

T.P.No.	AISI No.	Density (kg/m3)	Young's Modulus (GPa)			Poisson's Ratio		
			Ultrasonic Testing	Strain Gauge	Error (%)	Ultrasonic Testing	Strain Gauge	Error (%)
1-1	304	7945	200.9	199.3	-0.8	0.288	0.292	+1.39
1-2	304	7953	202.0	202.0	0.0	0.299	0.283	-5.35
1-3	304	7955	201.3	200.4	-0.45	0.290	0.285	-1.72
1-4	304L	7977	203.4	199.5	-1.92	0.284	0.277	-2.46
1-5	310S	7933	195.8	192.0	-1.94	0.289	0.292	+1.04
1-6	316	8007	199.2	204.8	+2.81	0.272	0.285	+4.78

Table 6. *Experimental values of density, Young's Modulus and Poisson's ratio*
Tabela 6: *Eksperimentalne vrednosti gustine, Jungovog modula i Poasonovog odnosa ultrasonic testing-ultrazvučno ispitivanje; strain gauge—merač naprezanja; error-greška*

4.3.3 Young's modulus

Fig. 4 shows the relation between experimental values and calculated ones of *E*. The calculated values were smaller than experimental ones, and a margin of error except T.P.No.5-2 (AISI type 310S in Table 2) was less than 5.7%. It seemed that a margin of error mainly depended on the lack of data concerning Young's modulus necessary for calculation. Especially, it was hard to find out data concerning phosphorus and sulfur.

4.3.3 Jungov modul

Sl. 4 prikazuje odnos između eksperimentalnih vrednosti i izračunatih za *E.* Izračunate vrednosti su bile manje od eksperimentalnih i margina greške osim za T.P.No.5-2 (tip AISI 310S u tabeli 2) je bila manja od 5,7%. Činilo se da je margina greške uglavnom vezana za nedostatak podataka za Jungov modul potrebnih za izračunavanje. Posebno je bilo teško saznati podatke koji se odnose na fosfor i sumpor.

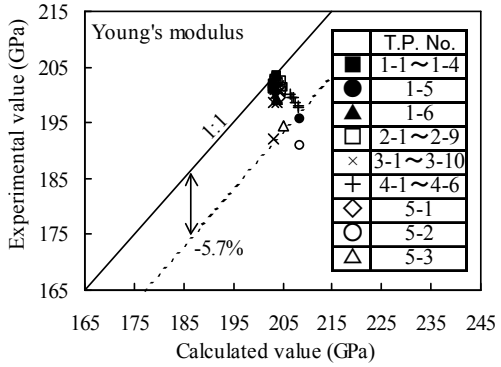

Fig. 4 *Relation between experimental values and calculated ones of Young's modulus*
Sl. 4. *Odnos između eksperimentalnih i izračunatih vrednosti za Jungov modul*

4.3.4 Poisson's ratio

Fig. 5 shows the relation between experimental values and the calculated ones of *v*. Calculated values were almost constant, and were independent of experimental ones. It seemed that a margin of error depended on the lack of data concerning Poisson's ratio of non-metallic elements such as carbon, phosphorus and sulfur.

4.3.4 Poasonov odnos

Sl. 5 prikazuje odnos između eksperimentalnih i izračunatih vrednosti za v. Izračunate vrednosti su gotovo konstantne, i bile su nezavisne od eksperimentalnih. Činilo se da margina greške uzrokovana nedostatkom podataka za Poasonov odnos nemetalnih elemenata kao što su ugljenik, fosfor i sumpor.

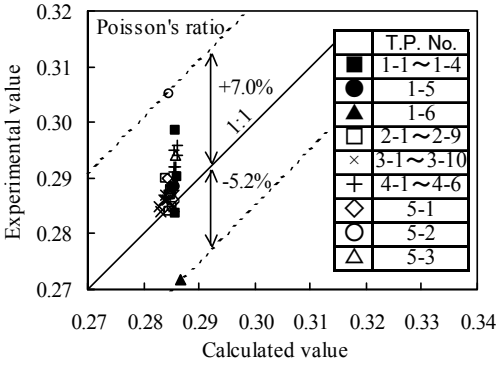

Fig. 5 *Relation between experimental values and calculated ones of Poisson's ratio*
Sl. 5. *Odnos između eksperimentalnih i izračunatih vrednosti Poasonovog odnosa*

4.3.5 Longitudinal wave velocity

Fig. 6 (a) shows the relation between experimental values and calculated ones of C_L. Since a margin of error was from 0.5% to -2.1%, we can say that longitudinal wave velocity of austenitic stainless steel would be able to be estimated within an allowable margin of error in accordance with the method shown in this paper.

4.3.5 Brzina longitudinalnog talasa

Sl. 6 (a) prikazuje odnos između eksperimentalnih i izračunatih vrednosti za C_L. S obzirom da je margina greške bila od 0,5% do -2.1%, možemo reći da će brzina longitudinalnog talasa austenitnog nerđajućeg čelika biti u mogućnosti da se proceni u okviru dozvoljene margine greške u skladu sa metodom prikazan u ovom radu.

4.3.6 Transverse wave velocity

Fig. 6 (b) shows the relation between experimental values and calculated ones of C_S. A margin of error except AISI type 310S stainless steel was from 0.2% to -2.2%, and a maximum error of AISI type 310S was -4.9%. It is necessary to reexamine the method for estimating transverse wave velocity of AISI type 310S. Hence, we can say that transverse wave velocity of austenitic stainless steel except AISI type 310S can be estimated within an acceptable margin of error in accordance with the method shown in this paper.

4.3.6 Brzina transverzalnog talasa

Sl. 6 (b) prikazuje odnos između eksperimentalnih i izračunatih vrednosti za C_S. Margina greške osim za AISI tip 310S nerđajući čelik je od 0,2% do -2.2%, a maksimalna greška za AISI tip 310S je -4.9%. Potrebno je preispitati metode za procenu brzine transverzalnog talasa za tip AISI 310S. Dakle, možemo reći da se brzina transverzalnog talasa austenitnog nerđajućeg čelika, osim za AISI tip 310S može proceniti u prihvatljivoj margini greške u skladu sa metodom prikazanom u ovom radu.

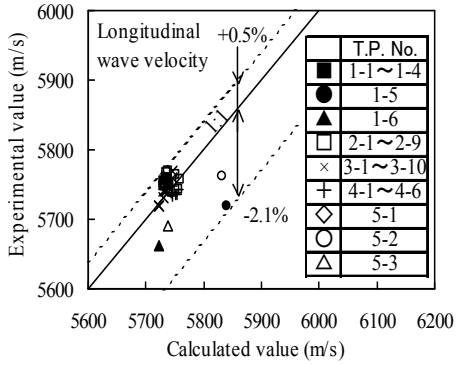

(a) Longitudinal wave velocity
(a) Brzina longitudinalnog talasa

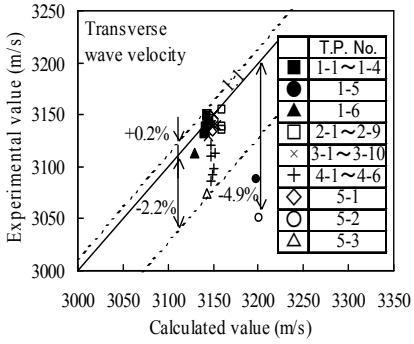

(b) Transverse wave velocity
(b) Brzina transverzalnog talasa

***Fig. 6** Relation between experimental values and calculated ones of ultrasonic wave velocity*
***Sl.6.** Odnos između eksperimentalnih i izračunatih vrednosti brzine ultrazvučnog talasa*

4.4 Behavior of Deviation

4.4.1 Deviation in longitudinal wave velocity

Fig. 7 shows the relation between longitudinal wave velocity and the ratio of a deviation in each parameter *ρ*, *E* and *v*in Eq. (1) to the value calculated by Eq. (1), based on the assumption that one of these parameters was variable and others were constant. Zero of the horizontal axis shows that each parameter is equal to experimental value and ratio of a deviation in each parameter is zero.

Longitudinal wave velocity increased with the increase in the deviation of *E* and *v*. On the contrary, *ρ* decreased with the increase in *ρ*. Curve of *ρ* and *E* was reversed, because Eq. (1) shows that longitudinal wave velocity is in proportion to a square root of *E*/*ρ*.

4.4 Ponašanje odstupanja

4.4.1 Odstupanje brzine longitudinalnog talasa

Sl. 7 prikazuje odnos između brzine longitudinalnog talasa i odnos odstupanja svakog parametra*ρ, E i v* u jednačini. (1) od izračunatih vrednosti prema jedn. (1), zasnovan na pretpostavci da je jedan od tih parametara bio promenljiv a ostali su bili konstantni. Nula na horizontalnoj osi pokazuje da je svaki parametar jednak eksperimentalnoj vrednosti i da je odnos odstupanja u svakom parametru nula.

Brzina longitudinalnog talasa se povećava sa porastom odstupanja *E* i *v*. Naprotiv, *ρ* opada sa povećanjem *ρ*. Krive *ρ* i E su obrnute, jer jedn. (1) pokazuje da je brzina podužnog talasa proporcionalna kvadratnom korenu iz *E/ρ*.

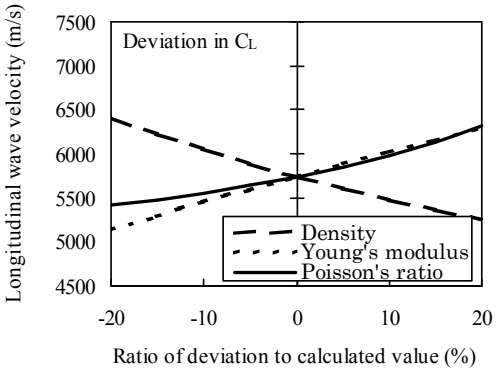

***Fig. 7** Relation between longitudinal wave velocity and ratio of deviation in factor of Eq. (1)*
***Sl. 7.** Odnos između brzine longitudinalnog talasa i odnos odstupanja faktora jedn. (1)*

4.4.2 Deviation in transverse wave velocity

Fig. 8 shows the relation between C_S and the ratio of a deviation of each parameterρ, E and v in Eq. (2) to the value calculated by Eq. (2). In Fig. 8, C_S decreased with the increase in a deviation of ρ and v, and increased with the increase in E, because Eq. (2) shows that transverse wave velocity is in proportion to a square root of E/ρ.

Comparing a curve of C_S with that of C_L, a deviation in C_S was definitely smaller than that in C_L, because $\sqrt{[1/(2(1+v))]}$ in Eq. (2) is smaller than $\sqrt{[(1-v)/((1+v)(1-2v))]}$ in Eq. (1). For example, when v= 0.288 (experimental value in Table 5) of T.P.No.1-1, $\sqrt{[1/(2(1+v))]}$ was 0.62 and $\sqrt{[(1-v)/((1+v)(1-2v))]}$ was 1.14.

4.4.2 Odstupanje brzine transverzalnog talasa

Sl. 8 prikazuje odnos između C_S i odnos odstupanja svakog parametra ρ, E i v u jednačini. (2) od izračunatih vrednosti prema jedn. (2). Na sl. 8, C_S je smanjen sa povećanjem odstupanja ρ *i* v, a raste sa povećanjem E, jer jed. (2) pokazuje da je brzina transverzalnog talasa proporcionalna kvadratnom korenu iz E/ρ.

Upoređujući krivu C_S sa C_L, odstupanje C_S je definitivno manje nego C_L, jer $\sqrt{[1 / (2 (1 + v))]}$ u jednačini (2) je manje od $\sqrt{[(1-v) / ((1 + v) (1-2v))]}$ u jednačini (1). Na primer, kada je v = 0.288 (eksperimentalna vrednost u tabeli 5) za TPNo.1-1, $\sqrt{[1 / (2 (1 + v))]}$ je 0.62 i $\sqrt{[(1-v) / ((1+ v) (1-2v))]}$ je 1.14.

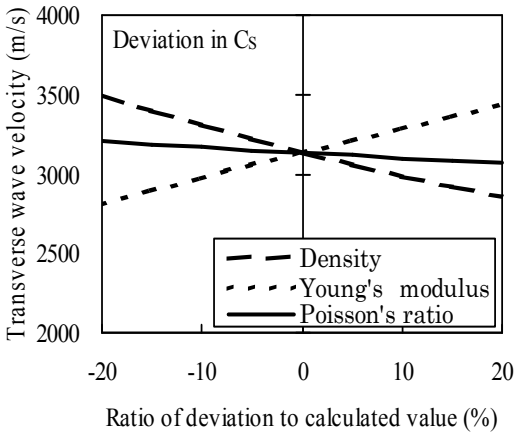

Fig. 8 *Relation between transverse wave velocity and ratio of deviation of parameter ρ, E andv in Eq.(2) to calculated value*

Sl. 8. *Odnos između brzine transverzalnog talasa i odnosa odstupanja parametara ρ, Eiv ujedn. (2) za izračunate vrednosti*

4.4.3 Deviation in density

Fig. 9 shows the relation between density and the ratio of a deviation in lattice parameter to that calculated by Eq. (5). In Fig.9, ρ increased rapidly with the decrease in a deviation in d.

4.4.3 Odstupanje gustine

Sl. 9 pokazuje odnos između gustina i odnos odstupanja parametra rešetke u odnosu na izračunate prema jedn. (5). Na sl.9, ρ je nagli porast pri smanjenju odstupanja d.

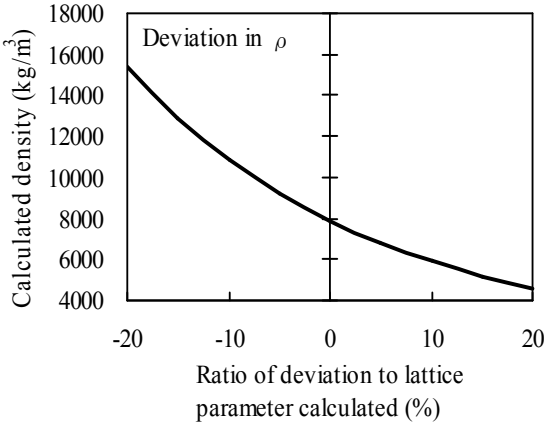

Fig. 9 Relation between density and ratio of deviation to lattice parameter calculated
Sl. 9. Odnos između gustine i odnosa izračunatog odstupanja parametra rešetke

4.4.4 Deviation in partial differentiation of *∂ρ/∂d* with regard to lattice parameter

Fig. 10 shows the relation between *∂ρ/∂d* and the ratio of a deviation in *d* to the calculated value.
In Fig. 10, *∂ρ/∂d* increased rapidly with the increase in a deviation in *d*. Since figures of *∂ρ/∂d* was minus, it seemed that the curve in Fig. 9 corresponded with the deviation of *∂ρ/∂d* in Fig. 10.

4.4.4 Odstupanje parcijalne diferencijacije *∂ρ/∂d* u odnosu na parametar rešetke

Sl. 10 pokazuje odnos između *∂ρ/∂d* i odnos odstupanja *d* prema izračunatoj vrednosti.
Na sl. 10, *∂ρ/∂d* je naglo poraslo sa porastom odstupanja *d*. S obzirom da su slike *∂ρ/∂d* bile u minusu, to znači da kriva na sl. 9 odgovara odstupanju *∂ρ/∂d* na sl. 10.

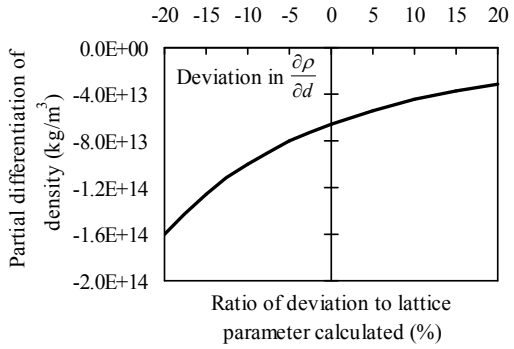

Fig.10 *Relation between ∂ρ/∂d and ratio of deviation to d*
Sl.10. *Odnos između ∂ρ/∂d i odnos odstupanjad*

4.4.5 Deviation in partial differentiation of *∂C/∂ρ* with regard to density

Fig. 11 shows the relation between *∂C/∂ρ* and the ratio of a deviation to *ρ*. In this figure, zero at horizontal axis represents that a deviation in*ρ* of experimental value shown in Table 5 is zero. In Fig. 11, *∂C/∂ρ* of C_L increased moderately with the increase in the ratio of a deviation to *ρ*. On the other hand, *∂C/∂ρ* of C_S increased slightly with the increase in the ratio of a deviation to *ρ*.

4.4.5 Odstupanje parcijalne diferencijacije ∂C/∂ρ s obzirom na gustinu

Sl. 11 pokazuje odnos između ∂C / ∂ρ i odnos odstupanja *ρ*.. Na ovoj slici, nula na horizontalnoj osi predstavlja odstupanje *ρ* eksperimentalnih vrednosti prikazano u tabeli 5 koje iznosi nula. Na Sl. 11, ∂C / ∂*ρ* C_L raste umereno sa povećanjem odnosa odstupanja *ρ*. S druge strane, ∂C / ∂*ρ* C_S se blago povećava sa povećanjem odnosa odstupanja *ρ*.

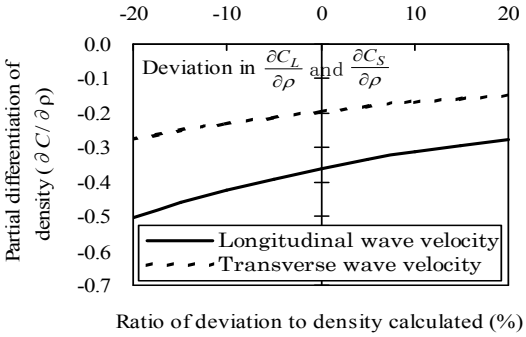

Fig.11 *Relation between ∂C/∂ρ and ratio of deviation to ρ*
Sl.11. *Odnos ∂C / ∂ρ i odnos odstupanja ρ*

4.4.6 Deviation in partial differentiation of *∂C/∂E* with regard to Young's modulus

Fig. 12 shows the relation between *∂C/∂E* and the ratio of a deviation in *E* to the calculated value.
Since *∂C/∂E* in Fig. 12 decreased with the increase in the ratio of deviation to *E*, the increment ofC_L in Fig. 7 and that of C_S in Fig. 8 decreased gradually.
In Fig. 12 the decrement of $\partial C_L/\partial E$ was larger than that of $\partial C_S/\partial E$.

4.4.6 Odstupanje parcijalne diferencijacije ∂C/∂E s obzirom na Jungov modul

Sl. 12 pokazuje odnos između ∂C/∂E i odnos odstupanja E prema izračunatim vrednostima.
S obzirom daje ∂C/∂E na sl. 12 smanjeno sa povećanjem odnosa odstupanja do E, prirast C_L na sl. 7 i dok C_S sa sl. 8 se postupno se smanjuje.
Nasl. 12 opadanje ∂CL/∂E je veće nego ∂CS/∂E.

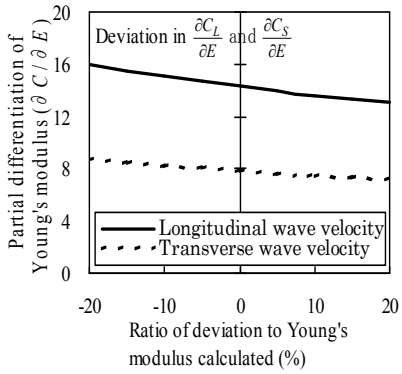

Fig.12 *Relation between ∂C/∂E and ratio of deviation to E*
Sl.12. *Odnos između ∂C/∂Ei odnos odstupanja E*

4.4.7 Deviation in partial differentiation of *∂C/∂v* with regard to Poisson's ratio

Fig. 13 shows the relation between *∂C/∂v* and the ratio of a deviation to *v*. In this figure, zero at horizontal axis represents that the deviation in *v* is zero. In Fig. 13 the increment of $\partial C_L/\partial v$ was considerably larger than that of $\partial C_S/\partial v$.

4.4.7 Odstupanje u parcijalne diferencijaciji ∂C / ∂v with obzirom na odnos Poissonov

Sl. 13 prikazuje odnos između ∂C/∂v i odnos odstupanja *v*. Na ovoj slici, nula na horizontalnoj osi predstavlja odstupanje v koje je nula. Na sl. 13 prirast ∂CL/∂v bio znatno veći od ∂CS/∂v.

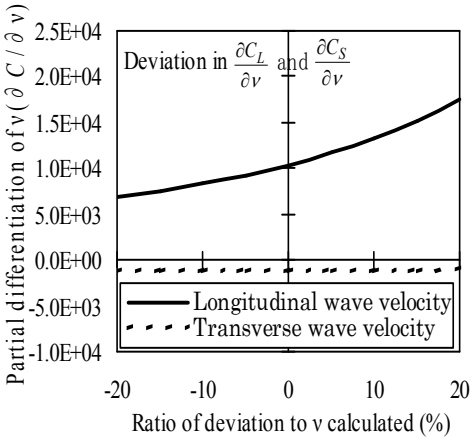

Fig.13 *Relation between ∂C/∂v and ratio of deviation to v*
Sl.13. *Odnos ∂C / ∂v i odnos odstupanjav*

5. Conclusions

(1) In calculating both lattice parameter and density by using chemical composition of material used, the calculated values were within an allowable margin of error, when assuming a few percent of error can be allowed, based on our experience. However, thecalculated values of Young's modulus and Poisson's ratio were beyond an allowable margin of error, because it was impossible to find out data of elementary substance.
(2) Acoustic anisotropy concerning transverse wave velocity ratio of T.P. No.1-1 ∼ 1-6 was not observed.
(3) The calculated value of longitudinal wave velocity were within an allowable margin of error.

5. Zaključci

(1) Pri izračunavanju i rešetke parametara i gustine, koristeći hemijski sastav materijala, izračunate vrednosti su bile unutar dozvoljenih margina greške, kada je pretpostavljeno da nekoliko procenata greške može biti dozvoljeno, na osnovu našeg iskustva. Međutim, izračunate vrednosti Jungovog modula i Poasonovog odnosa su bili van dozvoljene margine greške, jer je bilo nemoguće saznati podatke osnovne supstance.
(2) Akustična anizotropija vezana za odnos brzina transverzalnog talasa za T.P. No.1-1 ~ 1-6 nije uočena.
(3) Izračunata vrednost brzine longitudinalnog talasa su unutar dozvoljenih margina greške.

Similarly, the calculated values of transverse wave velocity except AISI type 310S stainless steel were within an allowable margin of error.
(4) The calculated value of density was gradually decreased with the increase in the ratio of a deviation in lattice parameter.
(5) Longitudinal wave velocity increased with the increase in a deviation of Poisson's ratio, and was in proportion to a square root of E/ρ.
(6) Transverse wave velocity decreased with the increase in a deviation of Poisson's ratio, and was in proportion to a square root of E/ρ.
(7) The deviation in longitudinal wave velocity due to the deviation of each parameters in Eqs. (1) and (2) was considerably larger than that in transverse wave velocity.

Slično tome, izračunate vrednosti brzina transverzalnog talasa, osim za AISI tip 310S nerđajućeg čelika su unutar dozvoljenih margina greške.
(4) Izračunata vrednost gustine je postepeno smanjena sa porastom odnosa odstupanja parametara rešetke.
(5) Uzdužna brzina talasa povećala s povećanjem odstupanje Poasonovog odnosa, i bio je u odnosu na kvadratni koren od E/ρ.
(6) Brzina transverzalnog talasa se smanjuje s povećanjem odstupanja Poasonovog odnosa, i proporcionalan je kvadratnom korenu iz E/ρ.
(7) Odstupanje brzine transverzalnog talasa zbog odstupanja svakog parametara u jednačinama (1) i (2) bio je znatno veći nego kod brzine transverzalnog talasa.

References
Literatura

1) Handbook for Non-destructive Inspection (New Version), Edited by The Japanese Society for Non-Destructive Inspection. Nikkan Kogyo Shimbun (1992), p.1283
2) H.M.Ledbetter, H.W.Austin ; Effect of Carbon and Nitrogen on the Elastic Constants of AISI Type 304 Stainless Steel, Materials Science and Engineering, 70(1985), p.143-149.
3) H.M.Ledbetter ; Manganese contributions on the elastic constants of face centred cubic Fe-Cr-Ni stainless steel, JOURNAL OF MATERIALS SCIENCE, 20(1985), p.2923-2929.
4) H.M.Ledbetter, S.A.Kim, J.Mater ; Molybdenum effect on Fe-Cr-Ni alloy elastic constants, Res.3(1), Jan/Feb (1988), p.40-44.
5) H.M.Ledbetter ; Sound velocities and elastic constants of steels 304, 310, and 316, Metal Science, December (1980), p.595-596.
6) Handbook of X-ray Diffraction, Rigaku, (2000), p.72-78
7) Material Data Book, Institute of Metallurgy in Japan, Maruzen, (2004), p.31, p.44.
8) W.C.Leslie ; Iron and Its Dilute Substitutional Solid Solutions. MATALLURGICAL TRANSACTIONS. Vol.3, January (1972), p.5-26.
9) S.Nishikawa ; Introduction of Material Engineering, Agne Gijutu Center (2001), p.92-96,
10) S.Nishikawa ; Introduction of Material Engineering, Agne Gijutu Center (2001), p.122,
11) S.Kohara ; Introduction of Metaragical Science, Asakura Shoten (2000), p.280-281.
12) Werner Köster ; H.Franz. et al. POISSON'S RATIO FOR METALS AND ALLOYS. METALLURGICAL REVIEWS. (1961), No.21, Vol.6, p.18-19.
13) R.M.German ; Science of Powder Metallurgy, Uchida Rokakuho (1996), p.524-529.